

## Quantum dynamics of a millikelvin quasibound KRb complex in a low-frequency field

J. S. Molano,<sup>1,\*</sup> K. D. Pérez,<sup>1,\*</sup> J. C. Arce<sup>ⓧ,1,†</sup> J. G. López<sup>ⓧ,1</sup> and M. L. Zambrano<sup>2</sup>

<sup>1</sup>*Departamento de Química, Universidad del Valle, A.A. 25360, Cali, Colombia*

<sup>2</sup>*Departamento de Ciencias Químicas, Universidad ICESI, Cali, Colombia*



(Received 28 March 2019; published 5 December 2019)

We investigate computationally the quantum dynamics of a metastable  $^{40}\text{K}^{87}\text{Rb}$  complex in the ground electronic state ( $X^1\Sigma^+$ ) under an intense continuous-wave low-frequency field. We focus on an initial condition where the atoms are quasibound in an orbiting resonance with an energy that corresponds to a kinetic temperature of 62 mK and with a lifetime of 3 ns. A microwave field is tuned either to another lower-lying orbiting resonance or to a high-lying bound vibrational level. In both cases, we observe a transient photoacceleration of the half-collision. However, the photodissociation of the complex is suppressed by strong quasibound-free Rabi oscillations, although it still dissociates nonradiatively with the lifetime of the initial orbiting resonance. During the transient period, a sizable multiphoton association in high-lying vibrational levels is achieved, accompanied by a development of a wide rotational distribution. Therefore, this mechanism seems promising as the basis of a general strategy for the controlled formation of diatomic molecules from gases at millikelvin temperatures.

DOI: [10.1103/PhysRevA.100.063407](https://doi.org/10.1103/PhysRevA.100.063407)

### I. INTRODUCTION

The formation of molecules in gases at very low temperatures is a research subject of growing interest in chemistry, molecular physics, and astrophysics [1]. In the laboratory, diatomic molecules have been obtained from cold ( $1\text{ mK} < T < 1\text{ K}$ ) and ultracold ( $T < 1\text{ mK}$ ) binary collisions by magnetoassociation and photoassociation (PA). In magnetoassociation, a Feshbach resonance between the colliding atoms is converted into a very weakly bound molecular level by tuning a magnetic field [2]. Such Feshbach molecule can subsequently be rovibrationally stabilized in the electronic ground state via stimulated Raman adiabatic passage or another control scheme [3]. In PA, once the colliding partners reach the Franck-Condon region or the so-called PA window, the diatom undergoes bound  $\leftarrow$  free absorption to a molecular electronic excited state followed by spontaneous or stimulated bound  $\rightarrow$  bound emission to a rovibrational level of the electronic ground state [4–6].

A simpler PA strategy would involve a direct free  $\rightarrow$  bound rovibrational transition in the electronic ground state. This kind of process was first studied computationally, employing a one-dimensional model, by Schmidt and coworkers, who showed that the final vibrational population can be controlled by means of an infrared (IR) subpicosecond laser pulse [7]. For cold and ultracold collisions, this strategy, which we will refer to as one-step PA (OSPA), has been envisioned with radio frequency (rf) [8], microwave (MW) [9], and IR [10,11] radiation. The fact that, for example, KRb Feshbach molecules have been formed with a rf field [12], and rf bound  $\rightarrow$  bound transitions have been utilized for vibrational stabilization of Rb<sub>2</sub> Feshbach molecules [13],

makes OSPA seem plausible. The simplicity of this strategy makes it very attractive, in particular because of its independence from excited electronic states and their associated short lifetimes, internal conversions, and intersystem crossings. Another advantage of OSPA is that control schemes can be devised to achieve PA together with vibrational stabilization with a single laser pulse [14,15]. However, it is limited to the formation of heteronuclear species, since the diatom must possess a dipole moment. An alternative strategy has been proposed, where an impulsive (short compared to the ultracold dynamics) light pulse creates a superposition that contains both scattering states of a purely repulsive electronic state and bound states of the ground electronic state [16].

These methods suffer from the limitation that the number of molecules produced is very low. In the case of PA, the efficiency is limited by the low density of atom pairs in the Franck-Condon region. Consequently, strategies involving the exploitation of resonances have been devised, which increase the formation probability of ultracold molecules by several orders of magnitude. One of them, called Feshbach-optimized photoassociation, employs resonances induced by a magnetic field or an electric field or a combination thereof [17]. Others employ scattering resonances, such as the adiabatic Raman PA [18], which enable PA at millikelvin temperatures [19]. In addition, it has been shown that nonresonant light with intensities of the order of  $10^{10}\text{ W cm}^{-2}$  can enhance the Boltzmann weight of orbiting (shape) resonances in a thermal ensemble and push scattering states below the dissociation threshold [20].

Schmidt and coworkers have also studied the effect of orbiting resonances on PA by IR laser pulses, taking into account the concomitant photoacceleration [21]. They have shown that these quasibound states can be used as initial states to selectively populate specific bound rovibrational levels. In this paper, we propose this process, which combines the above-mentioned advantages of OSPA and orbiting

\*These two authors contributed equally to this work.

†julio.arce@correounivalle.edu.co

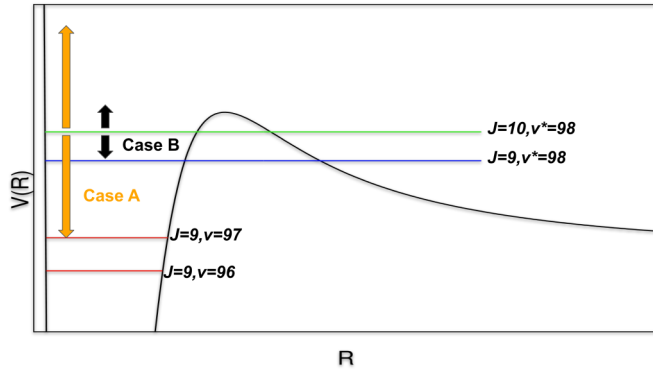


FIG. 1. Sketch of the radiative step in the OREOSPA mechanism. Only the high-energy region of the PEC, including the centrifugal contribution, is depicted. The energies of two orbiting resonances and two high-lying bound states are indicated. This figure is not drawn to scale and the PEC's, in particular the barrier heights, for different  $J$  are actually different.

resonances, as the basis of a strategy for the formation of rovibrationally cold and ultracold diatomic molecules from millikelvin atomic collisions, which we will refer to as orbiting resonance enhanced one-step PA (OREOSPA).

In Sec. II we explain the mechanism of OREOSPA and provide qualitative arguments for its plausibility as a strategy for the formation and control of cold and ultracold molecules. In Sec. III we present the working equations for the quantum dynamics of the nuclei and their diagnostics, and provide some details about the numerical methods used for implementing such equations and for calculating resonance properties. In Sec. IV we simulate the radiative step of OREOSPA in the formation of KRb, which is a widely used prototype of heteropolar molecule, from a millikelvin collision under an intense MW field. Our purpose here is not to model a specific situation that can be reproduced experimentally, but to gain insight into the dynamics of the process. In Sec. V we extract general conclusions from this work and point out future directions along this line of research.

## II. OREOSPA MECHANISM

OREOSPA can be conveniently visualized in terms of the mechanism



In the forward (f) step a metastable complex,  $(AB)^*(E', J')$ , where  $E', J'$  are the energy and rotational quantum number of an orbiting resonance, is formed by an elastic binary collision in the gas. The asterisk indicates a metastable collision complex. [We remind the reader that for  $J > 0$  the potential energy curve (PEC) develops a barrier (see Fig. 1) associated with the centrifugal contribution that appears in the radial equation (10). Such barrier may give rise to one or several orbiting resonances, which are quasibound states (see Fig. 2) with energies lying between the top of the barrier and the asymptotic value of the PEC.] Although

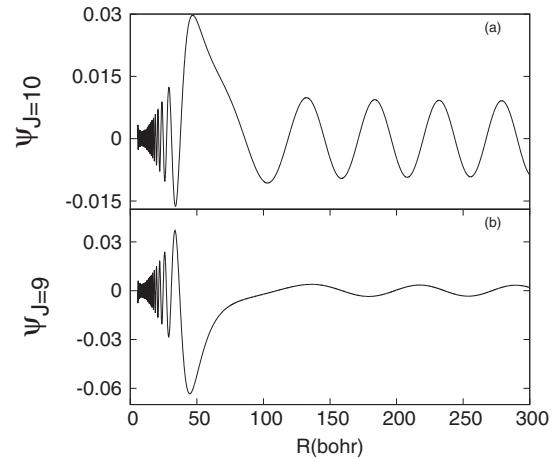


FIG. 2. Radial parts of the (a)  $J = 10, v^* = 98$  and (b)  $J = 9, v^* = 98$  resonance eigenfunctions.

in a cold thermal ensemble the scattering cross section is dominated by the  $s$ -wave component, there are significant populations in the resonances, whose contributions to the density of atom pairs in the inner region of the PEC delimited by the centrifugal barrier can be several orders of magnitude larger than the ones of all other  $J$  [22]. In the backward (b) step the complex decays by spontaneous nonradiative dissociation. In the radiative (rad) step the complex can be stabilized by stimulated emission into a molecular bound rovibrational level,  $AB(v'', J'')$ , or dissociated by absorption into a region of the continuum lying above the initial resonance. We consider two cases for the tuning of the applied field. In case A it is tuned to a high-lying bound vibrational level, in order to assess the feasibility of a direct PA. In case B it is tuned to a lower-lying resonance, in order to explore the possibility that such state serve as an intermediate channel for PA. These two cases are depicted in Fig. 1, where the downward and upward arrows refer to stimulated emission and absorption, respectively.

Most likely, the molecule will be formed in highly excited rovibrational levels, as these possess the highest resonance  $\rightarrow$  bound transition probabilities. Subsequently, the molecule can cascade down to low-lying levels via spontaneous emission [10], which is a very slow process, or be rovibrationally cooled by means of a control scheme [15]. For this mechanism to be efficient, the resonance  $\rightarrow$  bound transitions must be sufficiently strong and the resonances must get populated fast enough. In fact, another advantage of OREOSPA over plain OSPA is that resonance  $\rightarrow$  bound transitions are very much stronger than free  $\rightarrow$  bound transitions [23], as will be corroborated in Sec. IV. This avoids, in particular, the need to have the atoms tightly confined in an optical trap or lattice for an efficient association, as in Kotochikova's concept [9]. Furthermore, since the energies of many resonances correspond to kinetic temperatures in the millikelvin range, PA can be achieved with cold temperatures and IR fields, while plain OSPA requires ultracold temperatures and MW fields [9]. In fact, in lighter molecules the kinetic temperatures of the lowest-lying resonances can be as high as a few kelvin [23].

Naturally, resonance  $\leftarrow$  bound absorption from the field repopulates the resonances, which can ultimately lead to dissociation of the highly excited molecule, depending on the lifetimes of the resonances. In addition, in the absence of the field molecules can be formed by inelastic collisions of the complexes with free atoms, but these molecules can also be destroyed by collision-induced dissociation. Hence, a small equilibrium concentration of molecules in the gas is established. The point of applying the field is, precisely, to disrupt this equilibrium and generate a higher concentration of molecules.

In this paper, we address only the radiative step of mechanism (1), i.e., we assume that the complex is already formed. Moreover, we do not attempt to control this step, but consider a continuous-wave (CW) monochromatic radiation field. Under this condition, the neglect of the collisional step, which takes a relatively long time, is a reasonable approximation since the relevant dynamics takes place in the inner region of the PEC, where the magnitude of the dipole moment function is largest. A full treatment of this mechanism, under the nonequilibrium conditions of the field-dressed gas, necessitates a quantum kinetic model [24], which is beyond the scope of this work.

### III. METHODOLOGY

We consider a collision complex in the ground electronic state under a  $z$ -polarized field. The well-known dipole selection rules are  $\Delta J = \pm 1$  and  $\Delta M = 0$ . In the nuclear center-of-mass frame, we expand the nuclear wave function in partial waves,

$$\chi(R, \theta, \phi, t) = \sum_J \frac{1}{R} F_J(R, t) Y_J^0(\theta, \phi), \quad (2)$$

where we assumed that the initial state has  $M = 0$ . Within the semiclassical dipole approximation, the diatom-radiation interaction operator takes the form  $-d(R) \cos \theta \epsilon_0 \sin(\omega_0 t)$ , where  $d(R)$  is the dipole moment function of the diatom, and  $\epsilon_0$  and  $\omega_0$  are the amplitude and frequency of the field, respectively. The relative motion of the nuclei is governed by the system of equations

$$\begin{aligned} -i\hbar \frac{\partial}{\partial t} F_J(R, t) = & \left[ -\frac{\hbar^2}{2\mu} \frac{\partial^2}{\partial R^2} + \frac{\hbar^2 J(J+1)}{2\mu R^2} + V(R) \right] F_J(R, t) \\ & - \epsilon_0 \sin(\omega_0 t) d(R) [A_{J+1} F_{J+1}(R, t) \\ & + A_{J-1} F_{J-1}(R, t)], \end{aligned} \quad (3)$$

where  $\mu$  is the diatom reduced mass,  $V(R)$  is the Born-Oppenheimer PEC, and the angular factors are given by

$$A_{J+1} \equiv \frac{J+1}{[(2J+3)(2J+1)]^{1/2}} \quad (4a)$$

$$A_{J-1} \equiv \frac{J}{[(2J+1)(2J-1)]^{1/2}}. \quad (4b)$$

To diagnose the dynamics, we evaluate the expectation values of the total energy and its contributions, i.e., the radial kinetic energy, the potential energy, and the rotational energy,

$$\langle \hat{\Omega} \rangle(t) = \sum_J \langle F_J(t) | \hat{\Omega} | F_J(t) \rangle, \quad (5)$$

with  $\hat{\Omega} = -(\hbar^2/2\mu)d^2/dR^2$ ,  $V(R)$ ,  $\hbar^2 J(J+1)/2\mu R^2$ , respectively. We also evaluate the rotational distribution,

$$P_J(t) = |\langle F_J(t) | F_J(t) \rangle|, \quad (6)$$

the population of the initial resonance, i.e., the survival probability or autocorrelation function,

$$P_s(t) = |\langle \psi_{E',J'} | F_J(t) \rangle|^2, \quad (7)$$

where  $\psi_{E',J'}$  is the radial part of the eigenfunction of the initial resonance, the populations of the last and second-to-last vibrational levels of each  $J$ ,

$$P_{v,J}(t) = |\langle \psi_{v,J} | F_J(t) \rangle|^2, \quad (8)$$

and the trapping probability, defined as the contribution to the norm of the wave function from the inner region of the PEC,

$$P_{\text{trap}}(t) = \sum_J \int_0^{R_0} |F_J(R, t)|^2 dR, \quad (9)$$

where we chose  $R_0 = 76 a_0$ .

We used the KRb  $X^1\Sigma^+$  PEC reported in Ref. [25]. With this, we calculated the rovibrational bound and resonance states of  $^{40}\text{K}^{87}\text{Rb}$  by numerical integration of the radial equation,

$$\left[ -\frac{\hbar^2}{2\mu} \frac{d^2}{dR^2} + \frac{J(J+1)}{2\mu R^2} + V(R) - E_{v,J} \right] \psi_{v,J}(R) = 0, \quad (10)$$

employing the Colbert-Miller discrete-variable representation (DVR) [26]. Since the system is embedded in a box, the continuum energy becomes discretized and the continuum eigenfunctions become  $L^2$  integrable. In such a quasicontinuum, an index  $n$  can be introduced, such that the energies can be labeled as  $E(n)$  and a density of states (DOS) can be obtained as  $\rho(E) = (dE/dn)^{-1}$  (Ref. [27]). Such function may exhibit peaks, whose maxima are located at the energies of the shape resonances and whose full width at half-maxima,  $\Delta E$ , provide the lifetimes by  $\tau = \hbar/\Delta E$ . We implemented this scheme, evaluating the discrete derivative by means of a five-point (fourth-order) finite-differences formula. We adjusted the box size and the number of DVR points until we obtained convergence of the resonance energies to  $10^{-9}$  hartree, enough for our purposes. As a test of the accuracy of the integration method, we applied it to the bound states of a  $J = 0$  Morse oscillator fitted to resemble the PEC. We obtained agreement with the analytical results to  $10^{-13}$  hartree.

We employed the dipole moment function reported in Ref. [28]. With this, we computed resonance-resonance and resonance-bound dipole matrix elements (DMEs),

$$D(E', J'; E'', J'') = \langle \psi_{E',J'} | D | \psi_{E'',J''} \rangle, \quad (11a)$$

$$D(E', J'; v'', J'') = \langle \psi_{E',J'} | D | \psi_{v'',J''} \rangle, \quad (11b)$$

by numerical quadrature. For this calculation we enforced the appropriate Dirac-delta-like energy normalization [27] on the resonance eigenfunctions,  $\psi_{E,J}(R) = \rho^{1/2}(E) \tilde{\psi}_{E,J}(R)$ , where  $\langle \tilde{\psi}_{E,J} | \tilde{\psi}_{E,J} \rangle = 1$ . On the other hand, for the dynamical simulation the  $L^2$  eigenfunction of the initial resonance was taken normalized to unity,  $\tilde{\psi}_{E,J}$ , naturally.

We performed the numerical integration of the system of equations (3) on a grid whose points separate in an

TABLE I. Energies ( $E$ ), barrier heights (BH), and lifetimes ( $\tau$ ) of the selected orbiting resonances in the  $X^1\Sigma^+$  state of  $^{40}\text{K}^{87}\text{Rb}$ . Powers of 10 are indicated in square brackets.

$J$	$\nu^*$	$E$ (hartree, mK)	BH (hartree, mK)	$\tau$ (s)
9	98	9.1 [−8], 29	1.57 [−7], 49.5	7 [−9]
10	98	1.95 [−7], 61.8	2.11 [−7], 66.7	3 [−9]

exponential fashion, employing a fourth-order Runge-Kutta scheme [29]. This rather simplistic methodology allowed us to get converged and sufficiently accurate results with a manageable computation time.

#### IV. RESULTS AND DISCUSSION

Table I reports the energies, measured from the dissociation threshold, and the lifetimes of two selected orbiting resonances. For convenience of notation, these are assigned a fictitious vibrational quantum number,  $\nu^*$ , equal to the number of nodes displayed by the eigenfunction in the inner region of the PEC, such that the last bound vibrational level of the same  $J$  space has quantum number  $\nu = \nu^* - 1$ , and so forth. For convenience of reference, the heights of the centrifugal barriers and the kinetic temperatures,  $T = E/k_B$ , corresponding to the resonance energies and barrier heights are also reported in this table. We did not find resonances in  $J = 11$ . Figure 2 displays the radial parts of the eigenfunctions of these resonances. It is seen that the  $J = 9, \nu^* = 98$  resonance resembles more a bound state than the  $J = 10, \nu^* = 98$  resonance, as expected from their lifetimes.

We assume that the  $(^{40}\text{K}^{87}\text{Rb})^*$  complex is initially quibound in the  $J = 10, \nu^* = 98$  resonance. The applied field has an amplitude of  $\epsilon_0 = 10^{-3}$  atomic units. We consider two cases for the tuning of this field, as explained in Sec. II: In case A it is tuned to the  $J = 9, \nu = 97$  level, which is the last bound state for this  $J$ , and in case B it is tuned to the  $J = 9, \nu^* = 98$  resonance.

Table II reports the squares of the DMEs (11) and the energies for the one-photon transitions in cases A and B. For comparison purposes, it also reports these data for the transition between the last bound state of  $J = 10$  and the second-to-last bound state of  $J = 9$ . It can be seen that the resonance  $\leftrightarrow$  resonance transition (case B) is eight orders of magnitude stronger than the resonance  $\leftrightarrow$  bound transition (case A), which, in turn, is seven orders of magnitude stronger than the bound  $\leftrightarrow$  bound transition. This trend is observed in other systems as well [23]. Naturally, all these

TABLE II. Dipole matrix elements squared (DMES) and energies ( $E$ ) in atomic units for one-photon transitions. First line: case A. Second line: case B. Third line: bound-bound transition. Powers of 10 are indicated in parentheses.

Transition	DMES	$E$
$J = 10, \nu^* = 98 \leftrightarrow J = 9, \nu = 97$	1.509(+1)	9.32(−7)
$J = 10, \nu^* = 98 \leftrightarrow J = 9, \nu^* = 98$	1.927(+9)	1.04(−7)
$J = 10, \nu = 97 \leftrightarrow J = 9, \nu = 96$	3.469(−6)	1.95(−7)

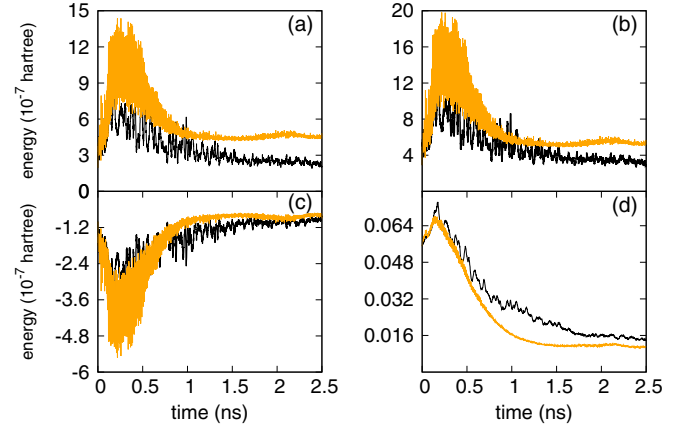


FIG. 3. Expectation value of the (a) total, (b) radial kinetic, (c) potential, and (d) rotational energy of the diatom. Orange (gray) line: case A. Black line: case B.

transitions are much stronger than free  $\leftrightarrow$  bound transitions. The frequencies of the case A and case B transitions are  $\approx 6$  GHz and  $\approx 0.7$  GHz, respectively, which fall deep in the MW region. We must point out that for these frequencies the field intensity used,  $I = 3.51 \times 10^{13} \text{ W cm}^{-2}$ , is at present unrealistically high from the experimental point of view. Considering that klystrons can achieve powers up to the order of  $10^8 \text{ W}$  [30], in the extreme case of a spot with the size of the wavelength ( $\sim 10 \text{ cm}$ ), an intensity of only  $\sim 10^6 \text{ W cm}^{-2}$  would be achieved. A realistic intensity for the MW region would likely be too low to produce observable effects in a computer simulation such as this. Intense IR fields can be used by tuning to lower-lying levels, but taking care that the DMEs are not too small. Since our goal here is to gain qualitative insight into the dynamics, we did not pursue this exploration.

Figure 3 displays the expectation values of the total, radial kinetic, potential, and rotational energy of the diatom [see Eq. (5)]. In both tuning cases, approximately during the first nanosecond there occurs a transient absorption of energy, with a larger absorption in case A. This amount of energy comprises mainly a kinetic energy gain and a lesser potential energy loss, which means that the (half-)collision accelerates, as has been observed in other OSPA studies [31]. After  $\sim 1.5$  ns the total energy attains an approximately steady behavior, in case A gaining a small net amount while in case B ending up with about the same value it began with. This photoacceleration may cause a heating of the gas. However, since most of the kinetic energy gain is transient and the gas is relatively dilute, the energy transfer between the complex and the gas should be inefficient, which implies that such heating is likely unimportant. The initial relative contribution of the rotational energy is very small. During the transient period, after a small gain this energy decreases to  $\approx 25\%$  of its initial value.

Figure 4 displays  $P_{J=10}(t)$  and Fig. 5 displays the  $P_{J\neq 10}(t)$  distributions for both tuning cases [see Eq. (6)]. During the transient period ( $\approx 1$  ns), a rapid loss of  $\approx 17\%$  of  $P_{J=10}$  is observed, with a concomitant rapid increase of the  $P_{J\neq 10}$ . Afterwards,  $P_{J=10}(t)$  continues decreasing while the  $P_{J\neq 10}(t)$  increase, now very slowly. After the transient period in case

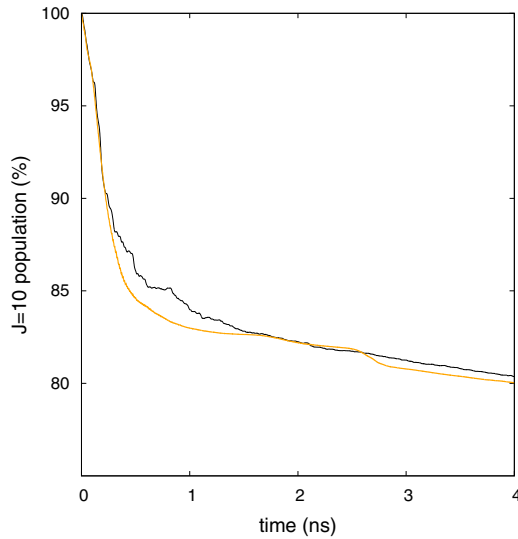


FIG. 4.  $J = 10$  population. Orange (gray) line: case A. Black line: case B.

At the  $P_{J \neq 10}$  distribution is biased towards  $J < 10$ , with the maximum at  $J = 8$ , whereas in case B it is biased towards  $J > 10$ , with the maximum at  $J = 13$ . Clearly, this means that during the transient period the system undergoes multiphoton rovibrational transitions, due to the high intensity of the field.

The top panel of Fig. 6 displays  $P_s(t)$  [see Eq. (7)] and Fig. 7 displays the  $P_{v,J}(t)$  [see Eq. (8)] for the last and second-to-last vibrational levels of all  $J$ , for both tuning cases. The  $P_s(t)$  are seen to exhibit strong Rabi-like oscillations with

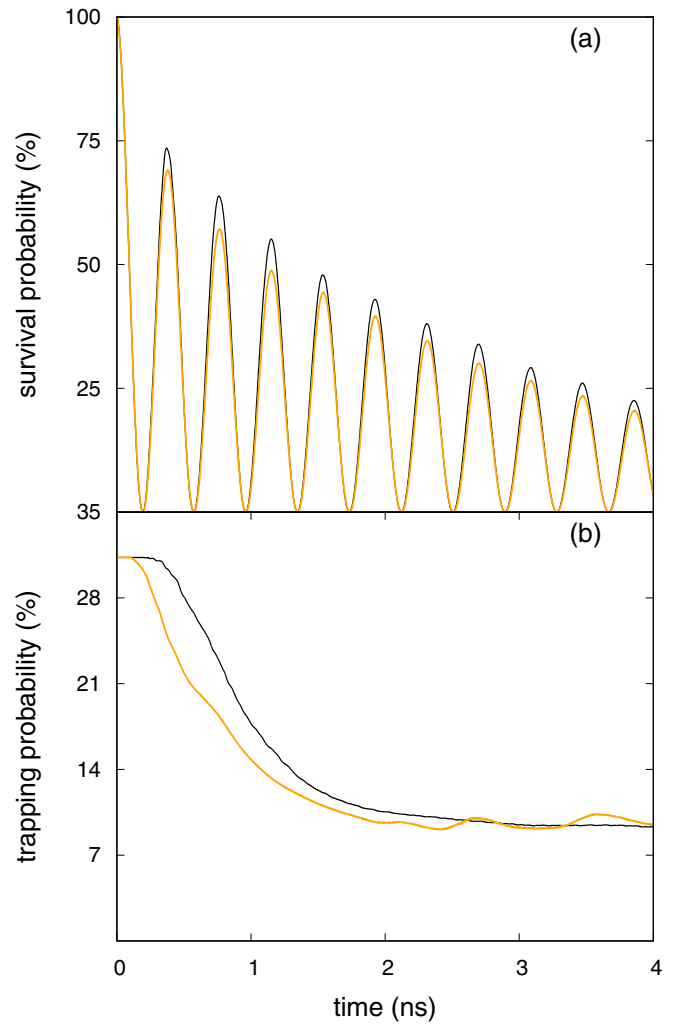


FIG. 6. (a) Survival probability. (b) Trapping probability. Orange (gray) line: case A. Black line: case B.

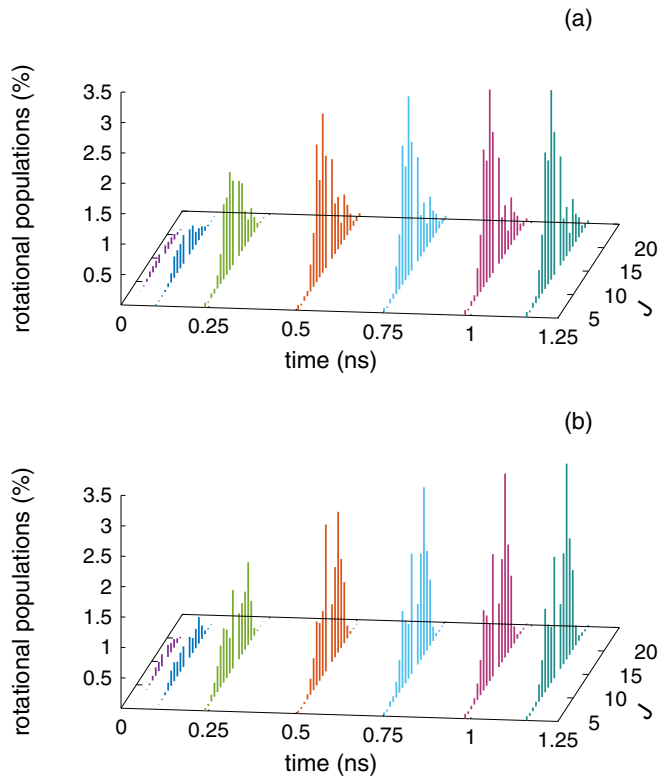


FIG. 5.  $J \neq 10$  distributions. (a) Case A. (b) Case B.

the same frequency  $\Omega \approx 4 \times 10^{-7}$  atomic units ( $\approx 17$  GHz) and nearly equal decaying amplitudes. Thus, it appears that the diatom is behaving like a two-level system, where one of the levels must be the  $J = 10$  quasibound state. In case A, the other level cannot be the  $J = 9$  last bound state, where the field is tuned, since its population does not exhibit the complementary Rabi oscillations, but instead remains practically zero at all times. This means that the  $J = 10$  quasibound state and the  $J = 9$  last vibrational level are not actually in resonance, due to the strong ac Stark shift. In fact, during the transient period the  $J = 10$  last vibrational level gets a population of up to about 3.3%, and the  $J = 6$  last and  $J = 10$  second-to-last vibrational levels get populations of up to about 0.5%. By the same token, in case B the population of the  $J = 9$  quasibound state (not shown) remains practically zero at all times, even though the field is tuned to it, whereas the  $J = 10$  last vibrational level gets about the same population as in case A, and the  $J = 9$  last and  $6 \leq J \leq 11$  second-to-last vibrational levels get populations within 0.3% and 1.2% during the transient period. These are also manifestations that the system is undergoing multiphoton rovibrational transitions.

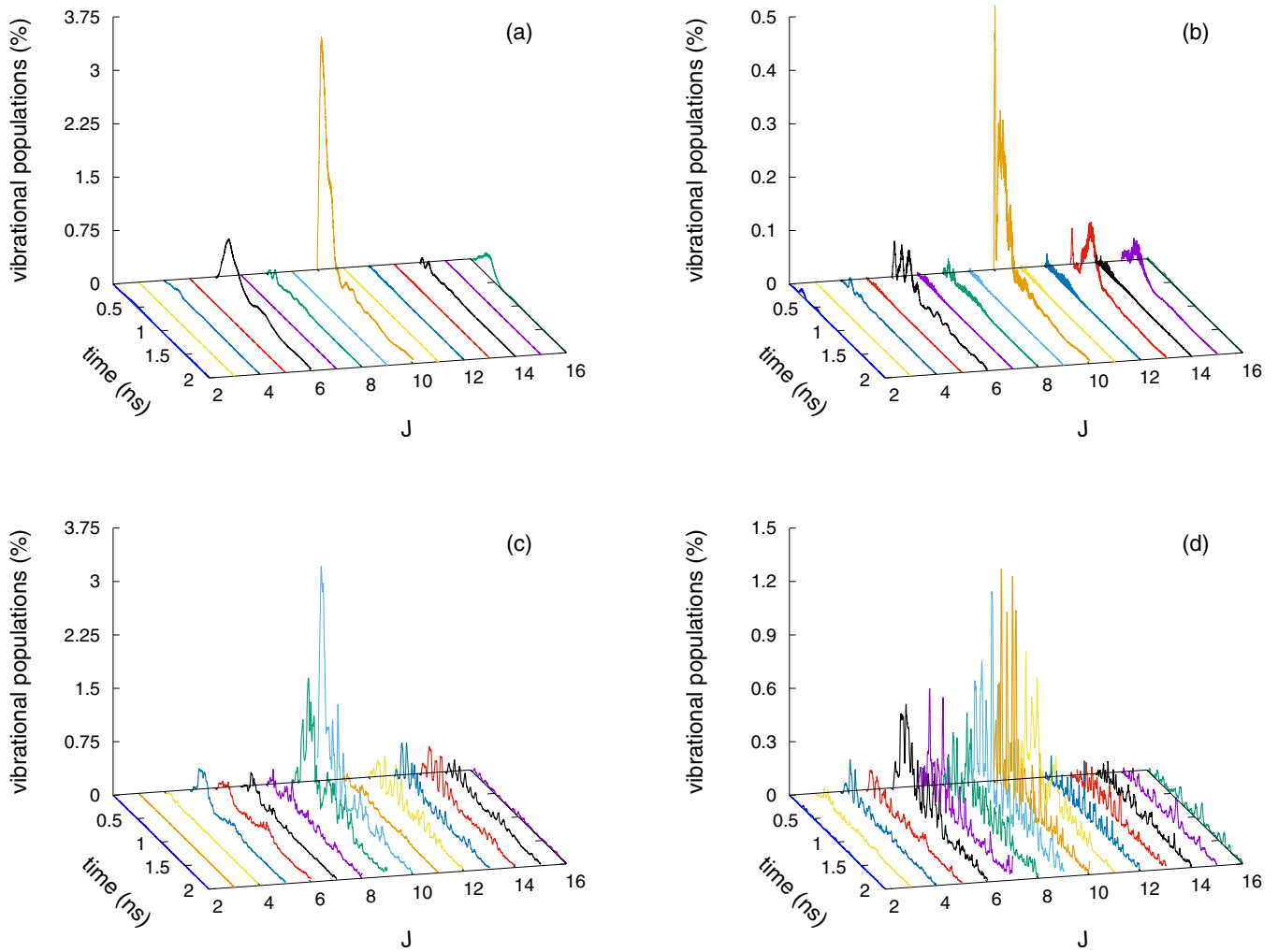


FIG. 7. Vibrational populations. (a) Last levels for case A. (b) Second-to-last levels for case A. (c) Last levels for case B. (d) Second-to-last levels for case B.

To understand the origin of the Rabi oscillations in the  $P_s(t)$ , we must take into account that in both tuning cases the initial quasibound state can simultaneously make, besides the rovibrational downward transitions, rovibrational upward transitions into the continuum above the centrifugal barriers (see Fig. 1). Let us consider a continuum  $\leftarrow$  quasibound absorption. If, hypothetically, the upper state were a discrete state, the Rabi frequency would be given by  $\Omega = \epsilon_0 \tilde{D}(E', J'; E'', J'') = \epsilon_0 D(E', J'; E'', J'') (\rho' \rho'')^{-1/2}$ , where  $\tilde{D}$  is the DME calculated with the eigenfunctions normalized to unity and  $\rho'$  and  $\rho''$  are the DOS's of the final and initial states, respectively. Taking into account the observation that  $\Omega_A = \Omega_B$  and recognizing that the continuum above a centrifugal barrier is largely unstructured, i.e., the DOS is relatively flat and the DME depends on the energy weakly, lead us to infer that the quasibound state is executing Rabi oscillations with a band of rovibrational states of the continuum above the centrifugal barriers. The plausibility of this interpretation is reinforced by the observation in computational studies of Rabi oscillations between a bound state and a continuum under a strong laser pulse [32], and bound-free and free-free Rabi oscillations involving vibrational levels of different electronic states of a diatomic molecule under strong laser pulses

[33,34]. Furthermore, this interpretation is in accordance with the rapid energy rise during the first  $\approx 0.2$  ns observed in the total and kinetic energies (see Fig. 3), which is about the time it takes  $P_s(t)$  to reach its first zero. As for the decay of the envelope of the oscillations, by means of an exponential fit we extract a decay constant of  $\approx 2.7$  ns, a little less than the initial resonance lifetime (3 ns). Hence, we infer that such decay is due mainly to the nonradiative decay of the complex [step (b) of mechanism (1)], with a small contribution from the nonresonant continuum. Transient time-dependent coherences have been observed in earlier computational and experimental studies, where short pulses were applied to nonresonant scattering states, generating bound vibrational wave packets in excited electronic states [35,36]. In the present case, the nature of the coherences, manifested as Rabi oscillations, is different, since the field is CW and only scattering states of the ground electronic state are involved. Moreover, their transient character is associated with the finite lifetime of the initial resonance, not with the dephasing of the wave packet.

The bottom panel of Fig. 6 displays  $P_{\text{trap}}(t)$  [see Eq. (9)] for both tuning cases. It is seen that initially  $\approx 32\%$  of the probability is trapped in the inner region of the PEC and, after

a short delay, which depends on the choice of  $R_0$ , in both cases it decays rather smoothly. An exponential fit yields a decay constant with the same value as the one of  $P_3$ , confirming that the decay is mainly nonradiative.

## V. CONCLUSIONS AND OUTLOOK

We have carried out a computer simulation of the radiative step of the OREOSPA mechanism (1) for a 62 mK metastable KRB complex, employing an intense MW field tuned directly to the high-lying bound vibrational region or to an intermediate orbiting resonance. Our findings can be summarized as follows. Even though the applied field is CW, the quasibound complex exchanges energy effectively with it during a transient period of  $\sim 1$  ns, which is shorter than the lifetime of the orbiting resonance (3 ns). Such exchange comprises mainly a kinetic energy gain, i.e., a photoacceleration of the half-collision. Nevertheless, the photodissociation of the complex is strongly suppressed by quasibound-free Rabi oscillations, so that the net dissociation is mainly nonradiative with the lifetime of the initial orbiting resonance. During the transient period a sizable multiphoton association in high-lying vibrational levels is achieved, accompanied by the development of a relatively wide rotational distribution.

We feel that the observed intense-field suppression of the photodissociation of the complex, through quasibound-free Rabi oscillations, is a very interesting phenomenon that warrants a more systematic and detailed investigation. In particular, the spectral characteristics of the diatom and the minimum field intensity that permit the onset of this phenomenon should be established.

The energy differences between the initial orbiting resonance and the high-lying bound vibrational levels selected, where the dipole coupling is strongest, is very small, so the field falls deep in the MW region. A higher frequency

range could be used by tuning the field to lower-lying levels, provided they possess strong enough couplings. In addition, collisions with energies above the centrifugal barriers can be considered. However, the direct coupling with the bound vibrational levels would now be much smaller. But we have observed that a lower-lying orbiting resonance can serve as an effective intermediate channel for photoassociation. Therefore, one can tune a field to such a state, which has a strong dipole coupling with the above-barrier continuum, to achieve a mediated photoassociation [37].

The OREOSPA mechanism can be supplemented by applying an additional strong static electric field. As has been shown in Refs. [11] and [38], such field can severely affect the stimulated emission process and be used to manipulate the vibrational structure of the molecule; in particular, high-lying bound states can be converted into resonances, which might also be used as channels for mediated millikelvin photoassociation.

Since it has been shown that an intense nonresonant field can push scattering states below the dissociation threshold [20], it is conceivable that the ac Stark shift stabilizes some of the lower-lying resonances and turns some of the scattering states into resonancelike states. Thus, if the initial resonance became a weakly boundlike state under the ac field, the aforementioned nonradiative decay would be suppressed as well. This conjecture is also worth further investigation.

Finally, we hope that our results will prove useful as guidance for the implementation of control schemes for the formation of ultracold molecules from millikelvin collisions by OREOSPA.

## ACKNOWLEDGMENT

This work was supported in part by Colciencias through Project No. 1106-658-42793.

- 
- [1] O. Dulieu and A. Osterwalder, *Cold Chemistry. Molecular Scattering and Reactivity Near Absolute Zero* (The Royal Society of Chemistry, Croydon, 2018).
- [2] V. Barbé, A. Ciamei, B. Pasquiou, L. Reichsöllner, S. Florian, P. S. Zuchowski, and J. M. Hutson, *Nature Phys.* **14**, 881 (2018).
- [3] R. D. Guerrero, M. A. Castellanos, and C. A. Arango, *J. Chem. Phys.* **149**, 244110 (2018).
- [4] W. C. Stwalley, P. L. Gould, and E. E. Eyler, in *Cold Molecules. Theory, Experiment, Applications*, edited by R. V. Krems, W. C. Stwalley, and B. Friedrich (CRC, Boca Raton, 2009), pp. 169–219.
- [5] J. Ulmanis, J. Deiglmayr, M. Repp, R. Wester, and M. Weidemüller, *Chem. Rev.* **112**, 4890 (2012).
- [6] D. Borsalino, B. Londoño-Flórez, R. Vexiau, O. Dulieu, N. Bouloufa-Maafa, and E. Luc-Koenig, *Phys. Rev. A* **90**, 033413 (2014).
- [7] M. Korolkov, J. Manz, G. K. Paramonov, and B. Schmidt, *Chem. Phys. Lett.* **260**, 604 (1996).
- [8] K. M. Jones, E. Tiesinga, P. D. Lett, and P. S. Julienne, *Rev. Mod. Phys.* **78**, 483 (2006).
- [9] S. Kotochigova, *Phys. Rev. Lett.* **99**, 073003 (2007).
- [10] E. Juarros, P. Pellegrini, K. Kirby, and R. Côté, *Phys. Rev. A* **73**, 041403(R) (2006).
- [11] R. González-Férez, M. Weidemüller, and P. Schmelcher, *Phys. Rev. A* **76**, 023402 (2007).
- [12] J. J. Zirbel, K.-K. Ni, S. Ospelkaus, T. L. Nicholson, M. L. Olsen, P. S. Julienne, C. E. Wieman, J. Ye, and D. S. Jin, *Phys. Rev. A* **78**, 013416 (2008).
- [13] F. Lang, P. V. D. Straten, B. Brandstätter, G. Thalhammer, K. Winkler, P. S. Julienne, R. Grimm, and J. H. Denschlag, *Nature Phys.* **4**, 223 (2008).
- [14] P. Marquetand and V. Engel, *J. Chem. Phys.* **127**, 084115 (2007).
- [15] E. F. de Lima, *J. Low Temp. Phys.* **180**, 161 (2015).
- [16] S. Kallush and R. Kosloff, *Phys. Rev. A* **77**, 023421 (2008).
- [17] X.-J. Hu, T. Xie, Y. Huang, and S.-L. Cong, *Phys. Rev. A* **89**, 052712 (2014).
- [18] A. C. Han, E. A. Shapiro, and M. Shapiro, *J. Phys. B: At. Mol. Opt. Phys.* **44**, 154018 (2011).
- [19] M. Wang, J.-L. Li, X.-J. Hu, M.-D. Chen, and S.-L. C. Cong, *Phys. Rev. A* **96**, 043417 (2017).

- [20] R. González-Férez and C. P. Koch, *Phys. Rev. A* **86**, 063420 (2012).
- [21] P. Backhaus, J. Manz, and B. Schmidt, *J. Phys. Chem. A* **102**, 4118 (1998).
- [22] C. P. Koch, R. Kosloff, E. Luc-Koenig, F. Masnou-Seeuws, and A. Crubellier, *J. Phys. B: At. Mol. Opt. Phys.* **39**, S1017 (2006).
- [23] K. D. Pérez, J. C. Arce, and J. G. López, *Astrophys. J. Suppl. Ser* **243**, 1 (2019).
- [24] R. C. Forrey, *J. Chem. Phys.* **143**, 024101 (2015).
- [25] A. Pashov, O. Docenko, M. Tamanis, R. Ferber, H. Knöeckel, and E. Tiemann, *Phys. Rev. A* **76**, 022511 (2007).
- [26] D. T. Colbert and W. H. Miller, *J. Chem. Phys.* **96**, 1982 (1992).
- [27] A. Macías, F. Martín, A. Riera, and M. Yáñez, *Int. J. Quantum Chem.* **33**, 279 (1988).
- [28] S. Kotochigova, P. S. Julienne, and E. Tiesinga, *Phys. Rev. A* **68**, 022501 (2003).
- [29] J. C. Tremblay and T. Carrington, Jr., *J. Chem. Phys.* **121**, 11535 (2004).
- [30] J. Benford, J. A. Swegle, and E. Schamiloglu, *High Power Microwaves*, 3rd ed. (CRC Press, Boca Raton, 2016).
- [31] M. V. Korolkov and B. Schmidt, *Chem. Phys. Lett.* **272**, 96 (1997).
- [32] E. Frishman and M. Shapiro, *Phys. Rev. A* **54**, 3310 (1996).
- [33] S. Magnier, M. Persico, and N. Rahman, *Phys. Rev. Lett.* **83**, 2159 (1999).
- [34] G. Granucci, S. Magnier, and M. Persico, *J. Chem. Phys.* **116**, 1022 (2002).
- [35] J. Mur-Petit, E. Luc-Koenig, and F. Masnou-Seeuws, *Phys. Rev. A* **75**, 061404(R) (2007).
- [36] F. Weise, A. Merli, F. Eimer, S. Birkner, F. Sauer, L. Wöste, A. Lindinger, W. Salzmann, T. G. Mullins, R. Wester, M. Weidemüller, R. Ađanođlu, and C. P. Koch, *J. Phys. B: At. Mol. Opt. Phys.* **42**, 215307 (2009).
- [37] J. S. Molano, Quantum dynamics of cold K-Rb collisions in the electronic ground state under a microwave field, Chemistry Thesis, Universidad del Valle, 2018.
- [38] R. González-Férez and P. Schmelcher, *New. J. Phys.* **11**, 055013 (2009).